J Biomol NMR (2011) 49:207–219
DOI 10.1007/s10858-011-9482-8

ARTICLE

Metabolic profiles show specific mitochondrial toxicities in vitro in myotube cells

Qiuwei Xu · Heather Vu · Liping Liu · Ting-Chuan Wang · William H. Schaefer

Received: 7 October 2010 / Accepted: 10 December 2010 / Published online: 26 February 2011

Abstract Mitochondrial toxicity has been a serious concern, not only in preclinical drug development but also in clinical trials. In mitochondria, there are several distinct metabolic processes including fatty acid β-oxidation, the tricarboxylic acid (TCA) cycle, and oxidative phosphorylation (OXPHOS), and each process contains discrete but often intimately linked steps. Interruption in any one of those steps can cause mitochondrial dysfunction. Detection of inhibition to OXPHOS can be complicated in vivo because intermediate endogenous metabolites can be recycled in situ or circulated systemically for metabolism in other organs or tissues. Commonly used assays for evaluating mitochondrial function are often applied to *ex vivo* or in vitro samples; they include various enzymatic or protein assays, as well as functional assays such as measurement of oxygen consumption rate, membrane potential, or acidification rates. Metabolomics provides quantitative profiles of overall metabolic changes that can aid in the unraveling of explicit biochemical details of mitochondrial inhibition while providing a holistic view and heuristic understanding of cellular bioenergetics. In this paper, we showed the application of quantitative NMR metabolomics to in vitro myotube cells treated with mitochondrial toxicants, rotenone and antimycin A. The close coupling of the TCA cycle to the electron transfer chain (ETC) in OXPHOS enables specific diagnoses of inhibition to ETC complexes by discrete biochemical changes in the TCA cycle.

Keywords NMR · Mitochondria · Toxicity · Metabolomics

Abbreviation

NMR	Nuclear magnetic resonance
FID	Free induction decay
WET	Water suppression enhanced through T1 effects
DSS-d6	2,2-dimethyl-2-silapentane-5-sulfonate sodium, or sodium 3-(trimethylsilyl)-1-propanesulfonate
DMSO	Dimethyl sulfoxide
LC–MS	Liquid chromatography-mass spectrometer
MRS	Magnetic resonance spectroscopy
TCA	Tricarboxylic acid
ETC	Electron transfer chain
PCr	Phosphocreatine
ATP	Adenosine triphosphate
ADP	Adenosine diphosphate
NADH	Reduced nicotinamide adenine dinucleotide
NAD^+	Nicotinamide adenine dinucleotide
$FADH_2$	Reduced flavin adenine dinucleotide
FAD^+	Flavin adenine dinucleotide
CoQ or Q	Coenzyme Q, or ubiquinone
$CoQH_2$	Ubiquinol
OXPHOS	Oxidative phosphorylation
OCR	Oxygen consumption rate
ECAR	Extracellular acidification rate
MPT	Mitochondrial permeability transition
LDH	Lactate dehydrogenase

Electronic supplementary material The online version of this article (doi:10.1007/s10858-011-9482-8) contains supplementary material, which is available to authorized users.

Q. Xu (✉) · H. Vu · L. Liu · W. H. Schaefer
Merck Research Laboratories, 770 Sumneytown Pike, West Point, PA 19486, USA
e-mail: qiuwei_xu@merck.com

T.-C. Wang
Merck Research Laboratories, 126 E. Lincoln Avenue, Rahway, NJ 07065, USA

Introduction

Mitochondria, ubiquitous organelles, are the powerhouses of eukaryotic cells. Energy stored in fatty acids, sugars, and even amino acids can be harvested by channeling their intermediate metabolites into mitochondria where they are used to generate the ultimate universal energy currency, ATP. ATP is exported outside mitochondria by abundant ATP/ADP antiporters in the inner mitochondrial membrane. Energy metabolism pathways operating inside mitochondria include fatty acid β-oxidation, Kreb's cycle (alternatively called the tricarboxylic acid (TCA) cycle), and oxidative phosphorylation (OXPHOS); these 3 pathways constitute a significant portion of the bioenergetics within a whole cell and they supply many intermediate metabolites that are used for the anabolism of amino acids and fatty acids outside the mitochondria. The amount of ATP generated in mitochondria inside individual cells depends on the number of mitochondria which is further dependent on the energy demand for the related tissues or organ. The number of mitochondria in a cell can vary depending on maturation and the age of the cell, tissue, and animal (Amacher 2005). The number of mitochondria usually ranges from hundreds to thousands per cell.

Inside mitochondria, the synthesis of ATP via the OXPHOS pathway is facilitated by coupling oxidation of NADH and $FADH_2$ with phosphorylation of ADP by ATP synthase. Inside mitochondria, NADH and $FADH_2$ are primarily generated from either the TCA cycle or fatty acid β-oxidation. Oxidation of NADH and $FADH_2$ results in transfer of electrons through electron transport complexes I to IV in the ETC that serves to reduce molecular oxygen to water, as well as release of protons. The high concentration of protons in the inter membrane space of the mitochondria sets up a concentration gradient across the inner membrane that drives the phosphorylation of ADP by the synthase—F_0F_1 ATPase complex. Some steps of the TCA cycle are in close proximity and intimately coupled to ETC in order to efficiently tie NADH and $FADH_2$ generation with electron extraction and transport. For example, in the inner mitochondrial membrane, dehydrogenation of succinate by succinate dehydrogenase is coupled to $FAD^+ \rightarrow FADH_2$ in complex II, and dehydrogenation of malate by malate dehydrogenase is coupled to $NAD^+ \rightarrow$ NADH in complex I. Such closely coupled TCA-OXPHOS conversions provide metabolomics with a unique opportunity to monitor and detect abnormalities or perturbation of the ETC and OXPHOS by measuring the changes to the profiles of endogenous metabolites involved in these processes.

Application of metabolomics to diagnoses of mitochondrial toxicities has been demonstrated in cases involving inhibition to fatty acid β-oxidation. For example, inhibition to fatty acid β-oxidation is noticed by the appearance of urinary short chain mono or di-carboxylic fatty acids (Mortishire-Smith et al. 2004, Vickers 2009), or plasma acylcarnitines (Chen et al. 2009). Inhibition or impairment to TCA-OXPHOS is often evaluated based on functions of isolated mitochondria from *ex vivo* tissues or in vitro cells; however, based on the close coupling between TCA and OXPHOS, metabolomics can also detect distinctive mitochondrial dysfunction due to genetic alteration to the complex enzymes or specific inhibition to particular ETC complexes by monitoring quantitative changes to TCA intermediate metabolites.

Metabolomics is the non-discriminative quantitative profiling of endogenous metabolites in living systems as small as cells or as intricate as animals or humans (Fiehn 2002, Nicholson et al. 2002, Robertson 2005, Wishart 2008, Xu et al. 2009). Currently, the profiling is generally done using NMR and LC–MS. Since most biomolecules contain hydrogens and the proton (^{1}H) has nearly 100% natural abundance and high sensitivity, ^{1}H-NMR is especially well suited for fast non-discriminative quantitative profiling based on a single internal quantification reference compound (Weljie et al. 2006, Xu et al. 2006, 2008). NMR analyses provide simple, convenient, and direct quantification of all detectable molecules in one single spectrum thanks to the universal response factor associated with protons. The universal response factor for protons with ^{1}H-NMR eliminates the need for individual reference standards (especially in stable isotope labels used with LC-MS) for absolute quantification. A chemical in an NMR spectrum does not generally display a single monolithic peak; rather, most chemicals display several multiplet NMR peaks with distinctive splitting patterns for individual protons. Unique characteristic peak patterns in NMR spectra can eliminate the need for tedious de novo structure determination for the tens to hundreds of endogenous metabolites that are often detected in each biological sample (Xu et al. 2006). However, such an approach requires establishment of an NMR reference library of all known and commercially available endogenous metabolites. The sensitivity for chemical detection by NMR is usually at the μM level; however, actual sensitivity for a biological sample can be improved by concentrating the sample, and implementing improved NMR technologies such as cryogenic probes and high magnetic fields.

Metabolomics-based analyses can readily detect mitochondrial toxicity or genetic disease without painstaking isolation of mitochondria (Shaham et al. 2010). If changes in metabolic profiles are indicative of underlying biochemical inhibition or impairment, metabolomic profiling can directly provide mechanistic information and diagnosis with tissue or cellular samples. If sensitivity and specificity are adequate for indicative metabolites, it can provide a routine diagnostic for toxicity and clinical screening based

on either cellular metabolites or ideally from accessible biofluids such as urine or plasma (Shaham et al. 2010). It can further play an important intermediate role in translating *ex vivo* measurements to potential in vivo magnetic resonance spectroscopy (MRS) diagnoses.

In this paper, we present an application of quantitative NMR to profile metabolites from in vitro cells, as well as culture medium from mouse C2C12 myotubes treated with two classical mitochondrial toxicants, rotenone and antimycin A that are specific inhibitors to complex I and complex III in the ETC, respectively (Fig. 1). Shaham et al. used these two toxicants to facilitate the search for small molecule biomarkers of mitochondrial impairment in myotube culture media as a prelude to in vivo diagnoses in human plasma samples from patients with genetic mitochondrial respiratory chain disorders (Shaham et al. 2010); their focus was limited to metabolites in extracellular culture media. Analyss of both intracellular metabolites and metabolites in culture medium are extremely important and helpful to understanding the mode of action for a therapeutic drug and investigating potential drug toxicities because not all endogenous metabolites can be readily excreted into culture media. A broad quantitative metabolic profile provides not only pathway inhibition but also its ultimate consequences to energy metabolites information such as ATP and phosphocreatine inside cells.

Materials and methods

Materials

All chemicals were purchased from Sigma–Aldrich (St. Louis, MO) unless otherwise noted. The deuterated aqueous buffers (80 mM potassium phosphate at pH = 7.0 with 2 mM DSS-d6) were purchased from Isotec (Miamisburg, OH, currently a subsidiary of Sigma–Aldrich).

Cell culture

Induction of mouse C2C12 myotubes from myoblast cells and treatments with rotenone and antimycin A are described in Shaham's paper (Shaham et al. 2010). In brief, the cell induction was carried out in 2% horse serum for 4 days. Cells in 10 ml DMEM culture media containing 4.5 mg/ml glucose were incubated for 8 h with either 0.1 μM rotenone or 0.5 μM antimycin A (DMSO, final concentration <0.1%), and the control cells were treated with an equivalent volume of DMSO. These conditions as well as two different toxicant concentrations were selected in order to approximately double lactate production by the treatments with rotenone and antimycin A, while still maintaining cell viability at the end of the incubation. Separate control cultures in the same medium, but without DMSO and the 2 toxicants, were incubated for 5 min, and they were used as the earliest time point references for quantitative comparison of endogenous metabolites. There were 8 replicates for each group. Cells were separated from culture media and quenched with dry ice cold 80% aqueous methanol to stop cellular metabolic activity and precipitate proteins. Supernatants of cell extracts and culture media were stored at −70°C prior to NMR analyses.

NMR analysis

Sample preparation for NMR

Samples were thawed at 4°C in a Eppendorf Thermomixer R with a mixing speed of 1,400 rpm. Aliquots of cell extract supernatants (250 μl containing approximately 1

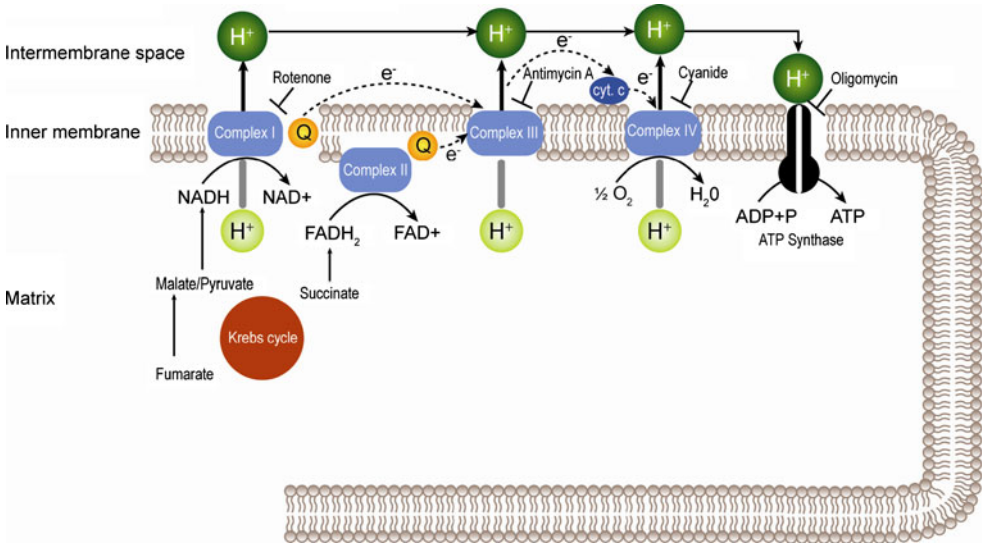

Fig. 1 Illustration of mitochondrial inhibition by rotenone and antimycin A, and coupling of TCA, or Krebs, cycle with ETC

million cells) were dried under nitrogen gas at the ambient temperature overnight. The dried cell extracts were admixed with 250 µl of 80 mM potassium phosphate buffer in 100% deuterium oxide containing 2.0 mM DSS-d_6, and mixed in an Eppendorf Thermomixer R at 1,400 rpm and at 10°C. Aliquots of culture media (125 µl) were admixed with 575 µl of 80 mM potassium phosphate buffer containing 2.0 mM DSS-d_6, and were mixed in an Eppendorf Thermomixer R at 1,400 rpm at 10°C. The solutions of cell samples were transferred to 4″ × 3 mm NMR tubes (Wilmad, Vineland, NJ), and culture media were transferred to 4″ × 5 mm NMR tubes. All NMR samples were placed in 8 × 12 NMR tube racks (Varian, Palo Alto, CA) on a Varian 768AS robot (Varian Inc., Palo Alto, CA) and kept at 8°C.

NMR instrument settings

One dimensional proton NMR spectra (1D ^{1}H-NMR) were acquired on a Varian ^{Unity}Inova 700 MHz NMR Spectrometry (Varian Inc., Palo Alto, CA) equipped with a cold probe and a 768AS robotic system. The probe temperature was set to 25°C. The 1D ^{1}H-NMR spectral width was 10,000 Hz, covering the range approximately from −2.37 to 11.91 ppm. The acquisition time was 3 s, corresponding to a digital resolution of 0.33 Hz. The water signal was suppressed with a WET1d pulse sequence that was based on selective excitation of the water peak using SINC pulses and gradient dephasing (Ogg et al. 1994). The selective excitation bandwidth (centered on the water peak) was 50 Hz. Transients of at least 256 scans were acquired with a relaxation delay of 15 s.

NMR data processing

Individual NMR FIDs (free induction decay) were apodized with a 0.2 Hz exponential line broadening, and extended to 64 k complex points before the Fourier transformation. NMR spectra were phased properly, and chemical shifts were referenced to the internal DSS-d_6 resonance (0 ppm). Spectra were saved for subsequent metabolite analyses using dataChord software (One Moon Scientific, Inc., Newark, NJ). Individual metabolites were identified based on a proprietary NMR reference spectrum library containing about 700 endogenous metabolites. Metabolite quantification was based on peak integration, and metabolite concentrations in NMR samples were calculated based on the area of the reference DSS-d_6 signal.

The concentration of metabolites in each NMR sample was expressed as fmoles per cell. The amounts of metabolites in culture media after 8 h incubation were compared to their reference samples at the earliest time point, and quantitative differences were used to calculate averaged rates of metabolism (net production or consumption) for individual metabolites. These rates were expressed as fmoles per cell and per hour.

The R statistical software (http://www.r-project.org) was used for statistical analyses based on non-parametric Wilcoxon pair-wise comparisons, and for making box and scatter plots.

Results and discussion

Overall NMR metabolic profiles

At least 41 endogenous metabolites in cell extracts and 30 chemicals in culture media were identified in 1D ^{1}H-NMR spectra (Figs. 2a, b, 3a, b, and Figures S1a and S1b in the supplemental materials). Pair-wise comparisons based on a non-parametric Wilcoxon rank test were performed on individual metabolites to evaluate their quantitative differences between any two of the three treatment groups (i.e., DMSO, rotenone, and antimycin A) for both cell lysates and culture media (Tables S1 and S2 in the supplementary materials). The comparison of cell lysates was based on the amounts of metabolites present in cells after the 8 h incubation, and the corresponding comparison of culture media was based on metabolic rates (i.e., net consumption or production rates in culture media as well as inside cells) of metabolites detected in culture media averaged over 8 h and the corresponding cell counts. Tables S1 and S2 display the results with a cutoff p-value of 0.05.

In cell lysates, biochemicals differentiating the treatment groups were fumarate, malate, and succinate, and thus quantitative levels of these three endogenous metabolites served as biochemical signatures in distinguishing these three treatment groups. High levels of succinate were associated with the antimycin A treatment (Fig. 2a), and high levels of malate and fumarate were associated with the rotenone treatment (Fig. 2b). Groups treated with antimycin A and rotentone were separated from the DMSO treatment group by changes in amino acids (e.g., alanine, glutamate, glutamine, proline, serine, and threonine), glucose, lactate, phosphocreatine, creatine, guanidineacetate, pantothenate, and α-glycerophosphorylcholine (Table S1 in the supplementary materials). These endogenous metabolites likely changed as a result of biochemical consequences to mitochondrial toxicities induced by antimycin A and rotenone. For example, cells treated with antimycin A or rotenone were found to contain higher amounts of alanine, serine, threonine, guanidineacetate, lactate, and creatine than did DMSO-treated cells; however, antimycin A- and rotenone-treated cells contained lower amounts of glutamine, glutamate, proline, pantothenate, phosphocreatine, and α-glycerophosphorylcholine than did those treated

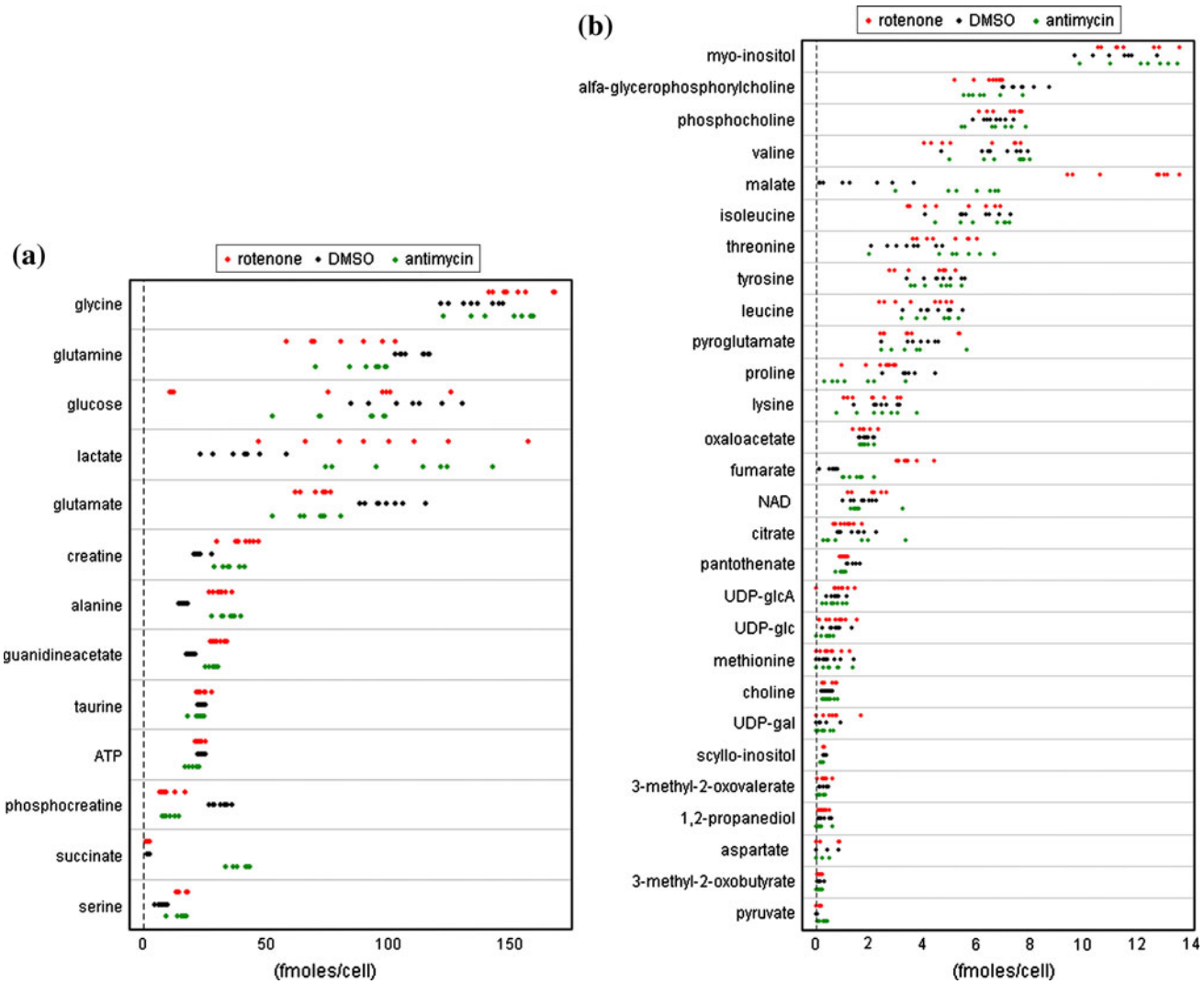

Fig. 2 **a** and **b** Scatter plots of metabolites (fmoles/cell) inside myotube cells treated with control (DMSO, *black solid circle*), rotenonre (*red solid circle*), and antimycin A (*green solid circle*)

with DMSO. Two endogenous metabolites, pyruvate and scyllo-inositol, distinguished the antimycin A group from the other 2 treatment groups (i.e., rotenone and DMSO groups). Antimycin A treated cells had higher pyruvate levels, but lower scyllo-inositol levels than did both rotenone and DMSO treated cells. Glycine seemed to differentiate the rotenone and DMSO treatment groups; rotenone treated cells contained higher amounts of glycine than did DMSO treated cells.

Metabolism rates for some metabolites detected in culture media also significantly differed among the treatment groups (Fig. 3a, b, and Table S2 in the supplemental materials). Biochemicals that displayed distinctively different metabolism rates among the three treatment groups included choline, citrate, formate, glucose, glycine, lactate, leucine, pyruvate, and serine. Treatment with rotenone and antimycin A increased glucose consumption, and propagated the increased production of lactate (Fig. 3a). Decreased expenditure of fed pyruvate (Fig. 3a) suggested that the observed lactate was derived mainly from glucose. Increased glucose consumption rates in cells treated with rotenone and antimycin A corresponded to decreased intracellular glucose levels (Fig. 5a), and reduced pyruvate consumption rates in culture media corresponded to increased intracellular pyruvate levels (Fig. 5b). Increased production of lactate led to its increased levels in cells (Fig. 5c). Between the two toxicants, antimycin A caused slightly less consumption of glucose and pyruvate, and, correspondingly, a reduced production of lactate compared to rotenone (Fig. 5a–c). Therefore, metabolites in or associated with the glycolysis pathway were perturbed in synchronicity; the production of terminal metabolites (e.g.,

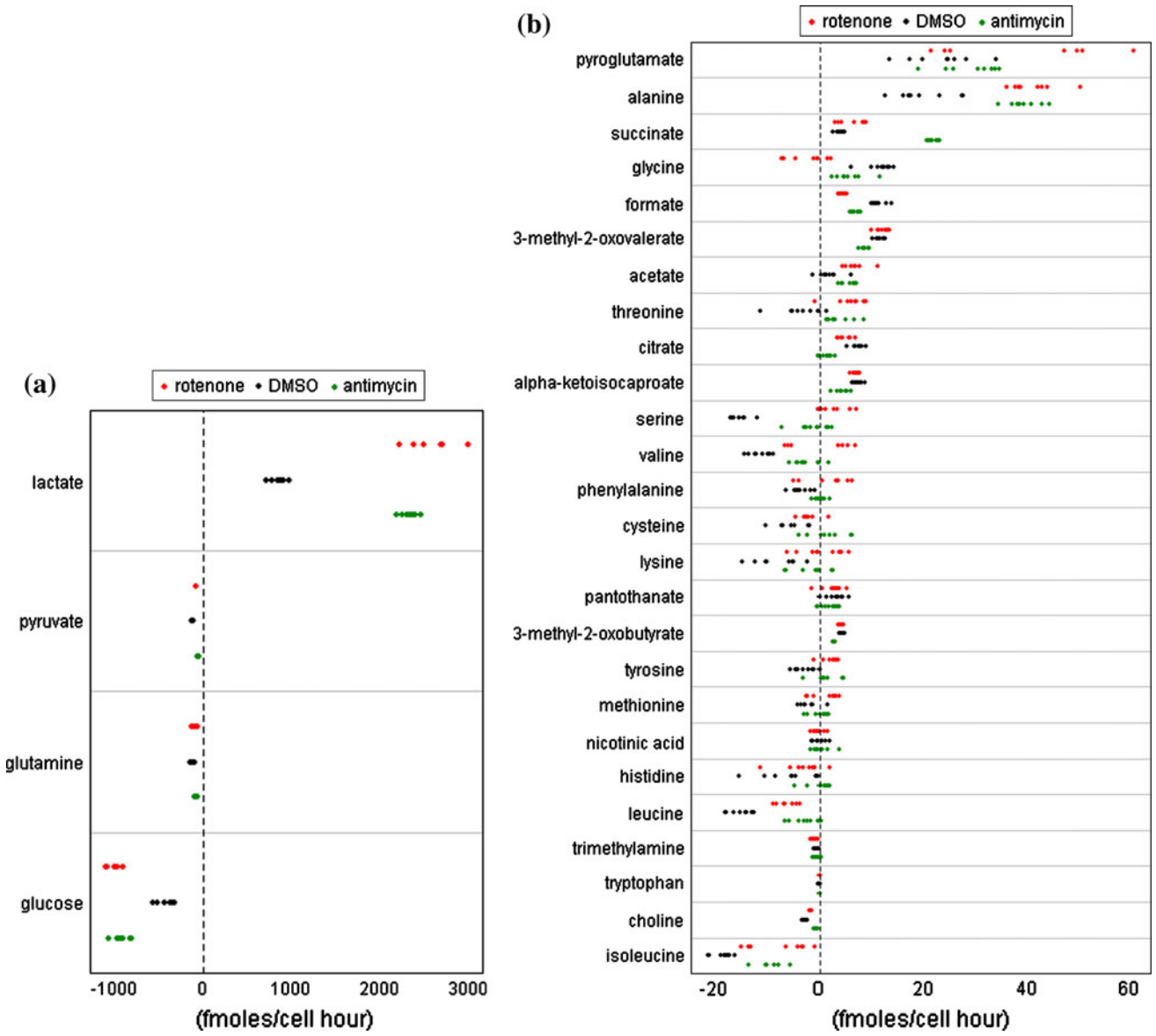

Fig. 3 **a** and **b** Scatter plots of metabolism rates (fmoles/cell hour) of listed metabolites in culture media of myotube cells treated with control (DMSO, *black solid circle*), rotenonre (*red solid circle*), and antimycin A (*green solid circle*)

pyruvate and lactate) was dictated by the consumption of starting metabolites (e.g., glucose).

Both rotenone and antimycin A reduced the production of formate and citrate (Figures S2a and S2b in the supplementary materials), but increased the production of acetate (Figure S2a in the supplementary materials). Antimycin A was associated with less production of citrate, but rotenone was associated with less production of formate. Reduction of citrate could suggest reduced activity of the TCA cycle that coupled closely to impaired OXPHOS; increased production of acetate could suggest breakdown of important intermediate metabolites such as acetyl-CoA. Both toxicants also caused reduced consumption of choline (Figures S2c in the supplementary materials); however, the consumption rate of choline was lower in cells treated with antimycin A than with rotenone.

The differentiation of treatments with rotenone and antimycin A from those treated with DMSO was further highlighted by changes in metabolism rates of amino acids (i.e., alanine, cysteine, isoleucine, leucine, lysine, methionine, phenylalanine, serine, threonine, tyrosine, and valine; Figures S3a-S3e in the supplementary materials, and Fig. 5e). Treatments with antimycin A and rotenone increased the production rates of alanine (Fig. 5e), but

reduced the consumption rates (small absolute values of negative rates) of the other amino acids, or turned net consumption to slight net production. Reduced consumption rates or slight net production of amino acids such as serine and threonine corresponded to their increased levels in cells (Figure S3c in the supplementary materials). Reduced consumption of amino acids might be instigated by the reduction of energy metabolites and their turnover rates. The increased production or changes from net consumption toward slight net production of amino acids could be due to cellular protein breakdown. The protein breakdown could be triggered by mitochondrial derailment. For example, the release of cytochrome c from mitochondria could trigger cell apoptosis. Analyses of their quantitative relationships, however, require further pathway flux analyses.

Cells treated with antimycin A were uniquely differentiated from those treated with rotentone and DMSO by increased production rates of succinate (Fig. 7), but reduced production rates of α-ketoisocaproate, 3-methyl-2-oxovalarate, 3-methyl-2-oxobutyrate, glutamine, and histidine (Figures S3a, S3b, and S3e in the supplementary materials). The increased production rate of succinate was consistent with its elevated concentration inside cells due to inhibition of complex III by antimycin A. α-Ketoisocaproate is a transamination metabolite of leucine; therefore, the reduced consumption rate of leucine and reduced production rate of α-ketoisocaproate indicated slowdown of leucine metabolism (Figure S3a in the supplementary materials). Both 3-methyl-2-oxobutyrate and 3-methyl-2-oxovalerate are coupled to valine by transamination; therefore, reduced consumption rates of valine and decreased output rates of 3-methyl-2-oxobutyrate and 3-methyl-2-oxovalerate suggested slowdown of cellular metabolism of valine (Figure S3b in the supplementary materials). Slightly decreased rates of amino acid metabolism due to antimycin A suggested that its inhibition at complex III instigated much stronger effect on overall cellular metabolism than did rotenone inhibit at complex I. To determine whether the slowdown in metabolism was due to cytochrome c release triggered by antimycin A inhibition requires further biochemical characterization (Ott et al. 2002).

Bioenergetic perturbation

The high potential energy of phosphoryl groups in muscle is mainly stored in the form of phosphocreatine (PCr). Phosphoryl groups in PCr are readily transferrable to ADP upon energy demand thanks to a favorable standard free-energy change in the conversion PCr + ADP → Cr + ATP. The standard free energy of the conversion is −3 kcal/mol, and it corresponds to an equilibrium constant of 162 (Stryer 1995). Storage of high energy phosphoryl groups in PCr can be illustrated by the steady state concentrations in typical type 2 muscles; the concentrations of PCr, ATP, and ADP are 32, 8 mM, and 8 μM, respectively, according to a publication by Kushmerick et al. (Kushmerick et al. 1992).

Treatments with rotenone and antimycin A caused PCr in myotube cells to decrease by almost 2/3 from its level in the DMSO control group (Fig. 4a) despite smaller decreases in ATP (Fig. 4b). There was a slight tendency for ATP to decrease in the rotenone treatment group as compared to the DMSO group; however, the decreases were statistically insignificant. The antimycin A treatment caused a noticeable ATP decrease with respect to the DMSO group. PCr was clearly more sensitive than ATP in reflecting a net loss of energy metabolites due to mitochondrial toxicity in myotube cells by its extreme susceptibility to energy depletion. Muscle cells appeared to maintain steady ATP concentrations by first trying to utilize and deplete PCr as the supply of high energy phosphate. It was reported that decreased ratios of PCr/ATP could be applied to predict mortality with dilated cardiomyopathy (Neubauer et al. 1997). In myotube cells, the PCr/ATP ratios decreased by at least half. The PCr/ATP ratio was approximately 1.31 in the DMSO control group,

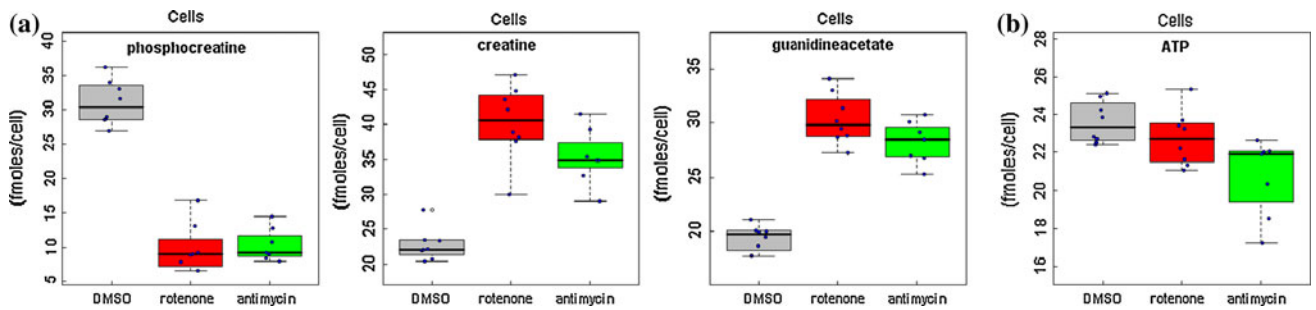

Fig. 4 **a** Boxplots of phosphocreatine, creatine, and guanidineacetate (fmoles/cell) in myotube cells treated with control (DMSO), rotenonre, and antimycin A. **b** Boxplots of ATP (fmoles/cell) in myotube cells treated with control (DMSO), rotenonre, and antimycin A

and it decreased to 0.42–0.50 in cells treated with rotenone or antimycin A.

Rotenone and antimycin A caused increases of both creatine and guanidinoacetate inside myotube cells (Fig. 4a). Guanidinoacetate methyltransferase (GMAT) catalyzes creatine biosynthesis by transferring a methyl group from S-adenosylmethionine to guanidinoacetate. The buildup of guanidinoacetate could be caused by product inhibition due to accumulation of creatine that was not phosphorylated due to the ETC inhibition. Excess guanidinoacetate is known to be neurotoxic. GMAT deficiency, an autosomal recessive genetic disease, was reported to impair the guanidinoacetate → creatine conversion, and it causes excess guanidinoacetate with concomitant creatine deficiency, that leads to neurodegeneration and muscle damage (Flynn et al. 2002, Schulze 2003, Schulze et al. 2003).

In the cell cultures used for this study, the main energy source was glucose. Glucose consumption rates were high but the intracellular glucose levels were low when myotube cells were treated with rotentone and antimycin A (Fig. 5a). The large disparity of glucose consumption rates in comparison to slightly reduced glucose levels inside cells when treated with rotenone and antimycin A suggested that glucose levels inside cells were maintained to be relatively stable presumably by unhindered glucose transporters in the plasma membrane. Despite the elevated consumption of glucose in cells treated with rotenone and antimycin A, it failed to maintain the normal PCr and ATP levels in cells (Fig. 4a, b). This is likely because the limited supply of ATP could have been derived only from glycolysis. The number of ATPs generated from each cycle of glycolysis is only 2, but further metabolism of the glycolysis end product, pyruvate, by the TCA and OXPHOS respiration processes in mitochondria can generate additional 34 ATP's. The interruption of mitochondrial respiration was indicated by the increased molar ratios of lactate produced relative to glucose consumed (Fig. 5d). The ratios of (produced) lactate/(consumed) glucose reached ~2.5 suggesting that externally fed pyruvate was not used appreciable by mitochondria. Instead, pyruvate was converted to lactate outside mitochondria when mitochondrial metabolism was inhibited by rotenone and antimycin A. Such diversion of pyruvate seemed to compensate for the failed recylcing of NADH → NAD^+. Inhibition of the ETC interrupted the recycling of reduced cofactors NADH and $FADH_2$ to oxidized NAD^+ and FAD^+, and pyruvate dehydrgenase requires NAD^+ for pyruvate metabolism to acetyl-CoA. The diversion of pyruvate → lactate by lactate dehydrogenase (LDH) helped to utilize the excess NADH and replenish the supply of NAD^+. Increased cellular lactate and its production rates (Fig. 5c) were the consequences of pyruvate → lactate diversion. Higher cellular pyruvate levels and its lower consumption rates from culture media due to treatment with 0.5 μM antimycin A, relative to 0.1 μM rotenone (Fig. 5b), indicated that 0.5 μM antimycin A exerted stronger inhibition to pyruvate uptake and utilization by mitochondria than did 0.1 μM rotenone.

Pyruvate can also be converted to alanine via transamination catalyzed by an aminotransferase through: pyruvate + glutamate → alanine + 2-ketoglutarate. Unlike the pyruvate → lactate conversion, the pyruvate → alanine transamination does not involve NADH → NAD^+ recycling; therefore, it does not directly help the need for NAD^+ in glycolysis by recycling NADH. Increases were seen in alanine levels in cells and its production rates while glutamate levels in cells decreased in the presence of rotenone and antimycin A (Fig. 5e). High cellular levels of lactate and its elevated production rates relative to those of alanine (Fig. 5c, e) suggested that a small portion of pyruvate was diverted to alanine.

Endogenous metabolite biomarkers specific to different mechanisms of mitochondrial toxicity

Rotenone and antimycin A inhibit OXPHOS in mitochondria at two different ETC complexes. Rotenone inhibits complex I by blocking electron transfer in NADH-Q reductase (Fig. 1), thus blocking proton transport from the mitochondrial matrix to the intermembrane space and inhibiting NADH → NAD^+ recycling. The oxidation of NADH → NAD^+ in ETC and malate → oxaloacetate in TCA, are closely coupled in mitochondria; therefore, interruption of NADH → NAD^+ led to accumulation of malate when myotube cells were treated with rotenone (Fig. 6). Malate is formed by hydration of fumarate in a freely reversible reaction catalyzed by fumarase, or fumarate hydratase (Wang et al. 1998). Accumulation of malate due to interruption of NADH → NAD^+, in turn, led to corresponding buildup of fumarate in rotenone-treated cells (Fig. 6).

Antimycin A interferes with electron flow in cytochrome reductase of mitochondrial complex III (Fig. 1). Mitochondrial complex III is coupled to complex II through $CoQH_2$ → CoQ that, in turn, facilitates $FADH_2$ recycling: $FADH_2$ → FAD^+. FAD^+ is involved in the conversion: succinate + FAD^+ → fumarate + $FADH_2$ in the TCA cycle. Therefore, inhibition to complex III by antimycin A impaired $FADH_2$/FAD^+ recycling and impeded the conversion of succinate to fumarate in the TCA cycle. As a consequence, there was high succinate accumulation inside the myotube cells treated with antimycin A (Fig. 7). The elevated production rates of succinate (Fig. 7) could be up-regulated by factors such as a feedback loop to compensate for decreases in energy metabolites. Slight increases of malate and fumarate (Fig. 6) in addition to

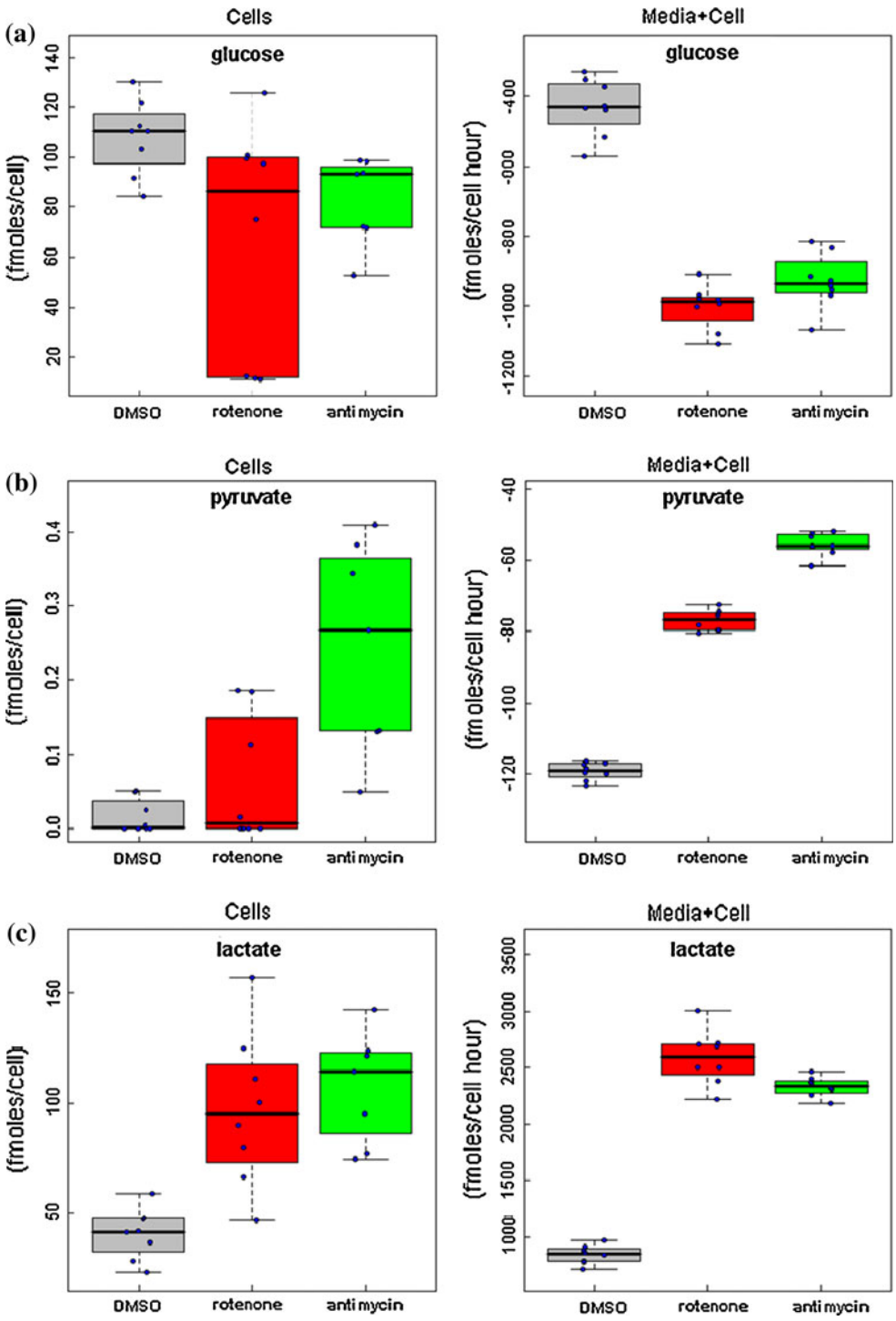

Fig. 5 **a** Boxplots of glucose inside myotube cells (*left*) (fmoles/cell) and its metabolism rates (fmoles/cell hour) in culture media and cell (*right*) when myotube cells were treated with control (DMSO), rotenonre, and antimycin A. **b** Boxplots of pyruvate inside myotube cells (*left*) (fmoles/cell) and its metabolism rates (fmoles/cell hour) in culture media and cell (*right*) when myotube cells were treated with control (DMSO), rotenonre, and antimycin A. **c** Boxplots of lactate inside myotube cells (*left*) (fmoles/cell) and its metabolism rates (fmoles/cell hour) in culture media and cell (*right*) when myotube cells were treated with control (DMSO), rotenonre, and antimycin A. **d** A box plot of the molar ratios of net produced lactate over net consumed glucose in culture media. **e** Boxplots of alanine inside myotube cells (fmoles/cell) and it metabolism rates (fmoles/cell hour) in culture media and cell, and glutamate in cells (fmoles/cell) when cells were treated with control (DMSO), rotenonre, and antimycin A

succinate caused by antimycin A were likely due to the propagating effects of inhibition of electron transport in complex III on complex I (Fig. 1). The blockage of the ETC at Complex III likely caused backing up of products associated with preceding complex II and decreased activity of Complex I.

Therefore, succinate was found to be specific to mitochondrial inhibition at complex II or III, and fumarate and malate were indicators of inhibition at complex I. These markers can supplement common mitochondrial functional assays, such as oxygen consumption, but also provide biochemical details of the inhibition.

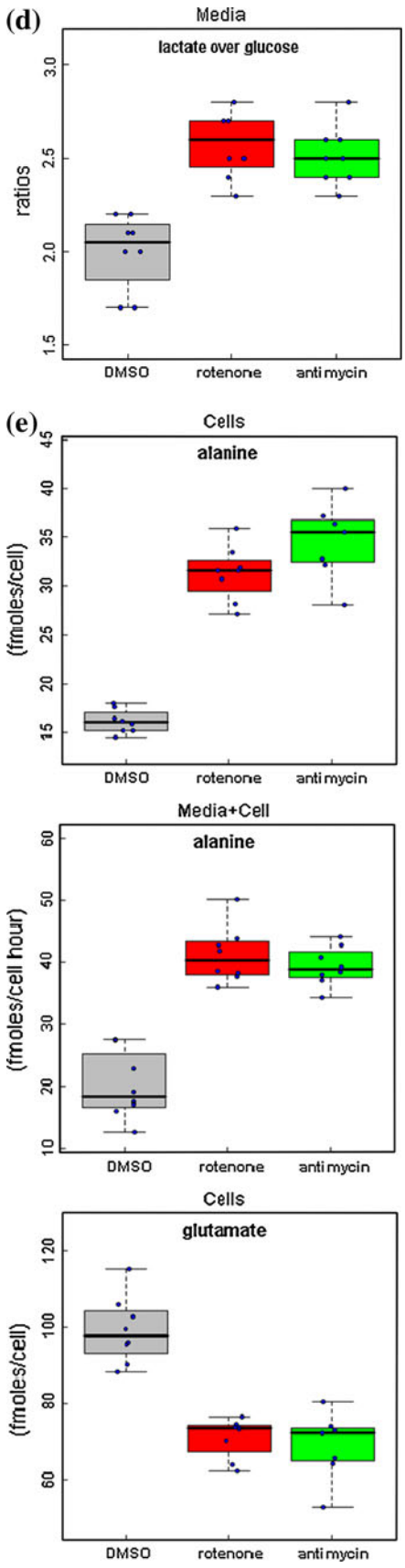

Fig. 5 continued

Changes of other endogenous metabolites specific to mitochondrial toxicities induced by rotenone and antimycin A

Citrate in the culture media changed in response to mitochondrial toxicity induced by rotenone and antimycin A, although its levels inside cells did not vary with the treatment (Figure S2b in the supplementary materials). The decrease in citrate production rates in culture media was much more pronounced in the presence of antimycin A.

The rate of consumption of choline from the culture media decreased significantly in response to rotenone and antimycin A treatment. However, the levels in the myotubes did not change with treatment (Figure S2c in the supplementary materials). Antimycin A almost totally blocked choline utilization while rotenone had a smaller effect.

Therefore, antimycin A was, in general, observed to exert a stronger influence to metabolism of citrate (Figure S2b in the supplementary materials), choline (Figure S2c in the supplementary materials), pyruvate (Fig. 5b), and succinate (Fig. 7) compared to rotenone.

Distinguishable metabolite profiles of mitochondrial toxicities

The above patterns of TCA cycle intermediate metabolites, including succinate, malate, and fumarate, in cell lysates (Figs. 6 and 7) were consistent with specific inhibition of OXPHOS complexes by rotenone and antimycin A (Fig. 1). Such characteristic changes in metabolite patterns provided useful biochemical details compared to other cell or mitochondrial assays. Most mitochondrial activity assays require mitochondrial isolation and the tests are often limited to mitochondrial function. These include measuring the oxygen consumption rate (OCR; Ferrick et al. 2008), extracellular acidification rate (ECAR; Ferrick et al. 2008), mitochondrial permeability transition (MPT; Amacher 2005, Nieminen et al. 2008), enzymatic activities of individual complexes I to IV (Birch-Machin 2008), and protein levels of complexes I-IV (Nadanaciva 2008). Endogenous metabolite profiling of cellular and culture media provides a straightforward methodology to observe metabolic changes associated with inhibition of biochemical pathways, and it complements those traditional mitochondrial assays. Traditional mitochondrial assays emphasize protein and enzymatic activities, but profiling of endogenous metabolites focuses on the substrates and products of those enzymatic processes. The responses from measuring proteins and metabolites are usually concordant, but sometimes they can be incongruous. For example, lack of intermediary metabolites, or co-factors, such as NADH or $FADH_2$, in the TCA cycle, may not be detected by enzymatic assays, but detection by metabolic profiling can

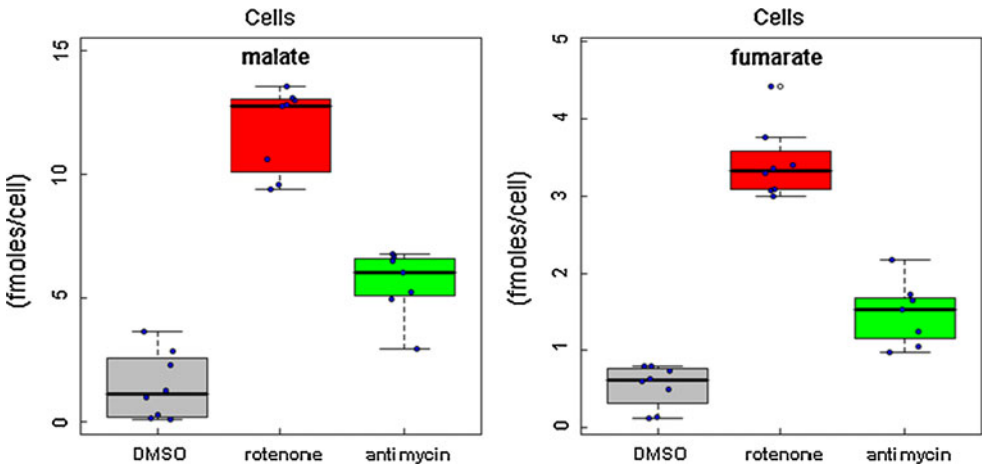

Fig. 6 Boxplots of malate and fumarate inside cells (fmoles/cell) when myotube cells were treated with control (DMSO), rotenonre, and antimycin A

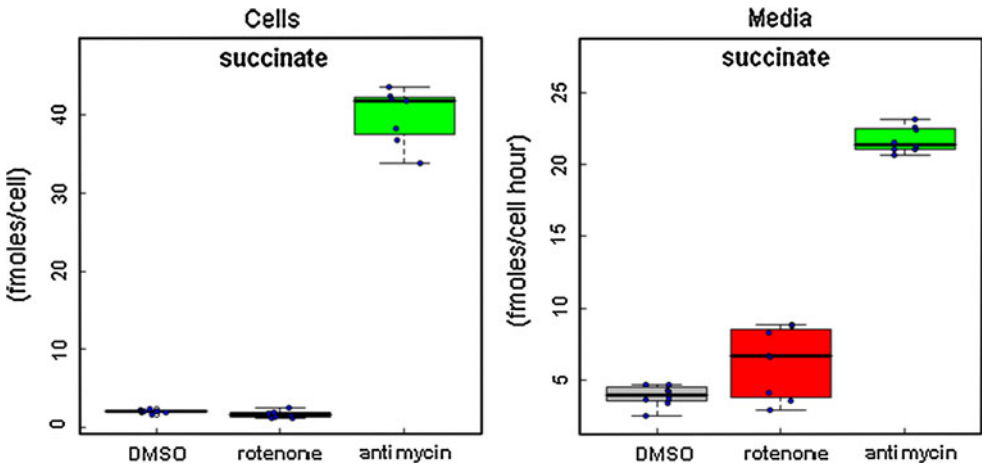

Fig. 7 Boxplots of succinate inside myotube cells (fmoles/cell) and its metabolism rates (fmoles/cell hour) in culture media when myotube cells were treated with control (DMSO), rotenonre, and antimycin A

provide the direct answer and valuable insight. On the other hand, enzymatic impairment detected using enzymatic assays should be supported by metabolic profiling. This shows the value of including metabolic profiling in the diagnosis of mitochondrial toxicity as a relatively simple but direct comprehensive readout.

Global metabolic profiling using metabolomics covers a wide range of endogenous metabolites, and it enables coherent understanding of changes to either endogenous metabolites or various metabolic pathways. The results in this study demonstrated that metabolic profiling not only detected specific inhibition of mitochondrial ETC complexes, but also displayed and confirmed corresponding impairment to other pathways associated with energy metabolism. Depletion of PCr and buildup of intermediary metabolites such as lactate, pyruvate, and alanine clearly showed that metabolite perturbations can be indicators or surrogates of ETC disruption and mitochondrial toxicity. Such potential causal relationships in metabolic processes were difficult to glean by observing only changes to proteins, transcripts, or genes alone. In this regard, absolute quantification of endogenous metabolites is a prerequisite to delineating intricate relationships of different metabolic pathways, for example, OXPHOS-TCA, glycolysis, and phosphorylation of creatine in the development of mitochondrial toxicity.

Different types of cells can have different rates of metabolism and numbers of mitochondria in each cell; therefore, their sensitivity toward mitochondrial toxicity can be variable. Extending the work in C2C12 cells here to other cell types in future should add to our basic understanding of mitochondrial toxicity. Cellular based metabolomics provides focused views with a wide metabolic perspective to biochemical mechanisms of mitochondrial toxicity. Measurements of both cellular concentrations of metabolites and metabolic rates of individual metabolite formation or utilization provide a more comprehensive characterization of cellular metabolism and mitochondrial toxicity.

Roles of profiling mitochondrial dysfunction in drug discovery and development

Detecting mitochondrial dysfunction and avoiding mitochondrial toxicity are crucial to drug discovery and

development. For example, Parkinson's disease has been linked to a deficiency of mitochondrion complex I activity in substantia nigra (Schapira et al. 1989). Inhibition of complex I by toxicants such as rotenone can lead to oxidative damage to the nigra due to increased free radical generation. This approach has been employed to chemically generate animal models for understanding the biochemical mechanisms and developing treatments for Parkinson's disease. Mitochondrial dysfunction in Parkinson's disease causes neurodegeneraton, and is linked to an over-expression of fibrillar α-synuclein aggregates (Lee 2003). Blocking an enzyme called SIRT2 was found to protect neurons from damage in Parkinson's disease by blocking the toxic effects of α-synuclein (Outeiro et al. 2007). Profiling bioenergetic metabolites should help evaluate the improvements of any treatment regimens, and could help facilitate the translation of such *ex vivo* assays to in vivo MRS in both preclinical and clinical settings (Ross et al. 2010).

Mitochondrial toxicity is often pernicious; therefore, drugs causing such adverse effects are often caught in preclinical tests, and thus rarely reach the market (Mortishire-Smith et al. 2004). In preclinical studies and even at early discovery stages, metabolomics can help, as illustrated in this paper, monitor and pinpoint biochemical mechanisms of mitochondrial dysfunction in addition to observing overall changes in metabolic pathways. This aids the selection of lead candidate compounds, and helps to guide the chemical design of improved compounds in order to avoid the mitochondrial toxicity.

Idiosyncratic cases sometimes appear in clinical trial phase IV, or post marketing surveillance trial. The nature of such toxicities is often very complicated due to the interplay of genetics, viral infections, pregnancy, and peculiar drug metabolism in the presence of compromised medical conditions (Pessayre et al. 2010). Mitochondria often become involved directly or indirectly in such late stage toxicities. Inhibition to OXPHOS can be induced, for example, in patients with pre-existing mitochondrial dysfunction such as a point mutation of mtDNA at an estimated rate of 1.6 in 10,000 Finnish population (Majamaa et al. 1998). Mitochondria are involved in pathways leading to either cell apoptosis or necrosis. Egress of cytochrome *c* from inner mitochondrial membrane can trigger apoptosis that requires sufficient supply of ATP; however, severe ATP depletion under such circumstances causes cell swelling and plasma membrane rupture, and ultimately leading to cell necrosis (Pessayre et al. 2010). Therefore, measurements of intracellular energy metabolites such as ATP are informative and valuable to distinguishing different pathways of cell death. Profiling endogenous metabolites related to mitochondrial energy metabolism should provide early warning signs for mitochondria-related toxicity, and help mitigate such undesirable effects by excluding patients who might be vulnerable to mitochondrial dysfunction.

Summary

Metabolomics of in vitro myotube cell samples showed metabolite changes that distinguished inhibition of mitochondrial oxidative phosphorylation by rotenone and antimycin A. Intimate coupling of the ETC and TCA cycle made it possible for metabolomics to detect inhibition to electron transfer in mitochondrial complexes by accumulation of intermediate metabolites in the TCA cycle. In addition, metabolomics confirmed the role of PCr to provide a phosphoryl buffer for ADP → ATP. ATP concentrations were maintained to be relatively stable although PCr levels were dramatically affected by mitochondrial toxicity in myotube cells. The advantages of metabolomics-based diagnoses of mitochondrial toxicity included avoiding the need for mitochondria isolation, detection of inhibition specific to individual ETC complexes, and a holistic view and heuristic understanding of metabolic processes and energy metabolism.

Acknowledgments We would like to thank Dr. Oded Shaham for his skilled preparation of the cell samples, and helpful suggestion of data analyses, and Drs. Eric Schadt, Vamsi Mootha, and Jun Zhu for facilitating the project. We feel grateful to Jill Williams for her superb artistic touch to Fig. 1. We appreciate Drs. Steven Pitzenberger and Frank Sistare for their critical reading of the manuscript.

References

Amacher DE (2005) Drug-associated mitochondrial toxicity and its detection. Curr Med Chem 12:1829–1839

Birch-Machin MA (2008) Assessment of mitochondrial respiratory complex function in vitro and in vivo. In: Will Y (ed) Drug-induced mitochondrial dysfunction. Wiley, London, pp 383–395

Chen C, Krausz KW, Shah YM, Idle JR, Gonzalez FJ (2009) Serum metabolomics reveals irreversible inhibition of fatty acid beta-oxidation through the suppression of PPARalpha activation as a contributing mechanism of acetaminophen-induced hepatotoxicity. Chem Res Toxicol 22:699–707

Ferrick D, Wu M, Swift A, Neilson A (2008) In: Will Y (ed) Drug-induced mitochondrial dysfunction. Wiley, London, pp 373–382

Fiehn O (2002) Metabolomics—the link between genotypes and phenotypes. Plant Mol Biol 48:155–171

Flynn NE, Meininger CJ, Haynes TE, Wu G (2002) The metabolic basis of arginine nutrition and pharmacotherapy. Biomed Pharmacother 56:427–438

Kushmerick MJ, Moerland TS, Wiseman RW (1992) Mammalian skeletal muscle fibers distinguished by contents of phosphocreatine, ATP, and Pi. Proc Natl Acad Sci USA 89:7521–7525

Lee SJ (2003) Alpha-synuclein aggregation: a link between mitochondrial defects and Parkinson's disease? Antioxid Redox Signal 5:337–348

Majamaa K, Moilanen JS, Uimonen S, Remes AM, Salmela PI, Karppa M, Majamaa-Voltti KA, Rusanen H, Sorri M, Peuhkurinen KJ, Hassinen IE (1998) Epidemiology of A3243G, the mutation for mitochondrial encephalomyopathy, lactic acidosis, and strokelike episodes: prevalence of the mutation in an adult population. Am J Hum Genet 63:447–454

Mortishire-Smith RJ, Skiles GL, Lawrence JW, Spence S, Nicholls AW, Johnson BA, Nicholson JK (2004) Use of metabonomics to identify impaired fatty acid metabolism as the mechanism of a drug-induced toxicity. Chem Res Toxicol 17:165–173

Nadanaciva S (2008) In: Will Y (ed) Drug-induced mitochondrial dysfunction. Wiley, London, pp 397–412

Neubauer S, Horn M, Cramer M, Harre K, Newell JB, Peters W, Pabst T, Ertl G, Hahn D, Ingwall JS, Kochsiek K (1997) Myocardial phosphocreatine-to-ATP ratio is a predictor of mortality in patients with dilated cardiomyopathy. Circulation 96:2190–2196

Nicholson JK, Connelly J, Lindon JC, Holmes E (2002) Metabonomics: a platform for studying drug toxicity and gene function. Nat Rev Drug Discov 1:153–161

Nieminen AL, Ramshesh VK, Lemasters JJ (2008) In: Will Y (ed) Drug-induced mitochondrial dysfunction. Wiley, London, pp 413–431

Ogg RJ, Kingsley PB, Taylor JS (1994) WET, a T1- and B1-insensitive water-suppression method for in vivo localized 1H NMR spectroscopy. J Magn Reson B 104:1–10

Ott M, Robertson JD, Gogvadze V, Zhivotovsky B, Orrenius S (2002) Cytochrome c release from mitochondrial proceeds by a two-step process. Proc Natl Acad Sci USA 99:1259–1263

Outeiro TF, Kontopoulos E, Altmann SM, Kufareva I, Strathearn KE, Amore AM, Volk CB, Maxwell MM, Rochet JC, McLean PJ, Young AB, Abagyan R, Feany MB, Hyman BT, Kazantsev AG (2007) Sirtuin 2 inhibitors rescue alpha-synuclein-mediated toxicity in models of Parkinson's disease. Science 317:516–519

Pessayre D, Mansouri A, Berson A, Fromenty B (2010) Mitochondrial involvement in drug-induced liver injury. Handb Exp Pharmacol 196:311–365

Robertson DG (2005) Metabonomics in toxicology: a review. Toxicol Sci 85:809–822

Ross JM, Oberg J, Brene S, Coppotelli G, Terzioglu M, Pernold K, Goiny M, Sitnikov R, Kehr J, Trifunovic A, Larsson NG, Hoffer BJ, Olson L (2010) High brain lactate is a hallmark of aging and caused by a shift in the lactate dehydrogenase A/B ratio. Proc Natl Acad Sci USA 107:20087–20092

Schapira AH, Cooper JM, Dexter D, Jenner P, Clark JB, Marsden CD (1989) Mitochondrial complex I deficiency in Parkinson's disease. Lancet 1:1269

Schulze A (2003) Creatine deficiency syndromes. Mol Cell Biochem 244:143–150

Schulze A, Bachert P, Schlemmer H, Harting I, Polster T, Salomons GS, Verhoeven NM, Jakobs C, Fowler B, Hoffmann GF, Mayatepek E (2003) Lack of creatine in muscle and brain in an adult with GAMT deficiency. Ann Neurol 53:248–251

Shaham D, Slate NG, Goldberger O, Xu Q, Ramanathan A, Souza AL, Clish CB, Sims KB, Mootha VK (2010) A plasma signature of human mitochondrial disease revealed through metabolic profiling of spend media from cultured muscle cells. Proc Nat Acad Sci USA 107:1571–1575

Stryer L (1995) Biochemistry. W.H. Freeman and Company, New York

Vickers AE (2009) Characterization of hepatic mitochondrial injury induced by fatty acid oxidation inhibitors. Toxicol Pathol 37:78–88

Wang X, Gong CS, Tsao GT (1998) Production of L-malic acid via biocatalysis employing wild-type and respiratory-deficient yeasts. Appl Biochem Biotechnol 70–72:845–852

Weljie AM, Newton J, Mercier P, Carlson E, Slupsky CM (2006) Targeted profiling: quantitative analysis of 1H NMR metabolomics data. Anal Chem 78:4430–4442

Wishart DS (2008) Quantitative metabolomics using NMR. Trends Anal Chem 27:228–237

Xu Q, Sachs JR, Wang TC, Schaefer WH (2006) Quantification and identification of components in solution mixtures from 1D proton NMR spectra using singular value decomposition. Anal Chem 78:7175–7185

Xu EY, Perlina A, Vu H, Troth SP, Brennan RJ, Aslamkhan AG, Xu Q (2008) Integrated pathway analysis of rat urine metabolic profiles and kidney transcriptomic profiles to elucidate the systems toxicology of model nephrotoxicants. Chem Res Toxicol 21:1548–1561

Xu EY, Schaefer WH, Xu Q (2009) Metabolomics in pharmaceutical research and development: metabolites, mechanisms and pathways. Curr Opin Drug Discov Devel 12:40–52